Volume 7
Number 5
9 March 2026
Pages 2511–3020

Materials Advances

rsc.li/materials-advances

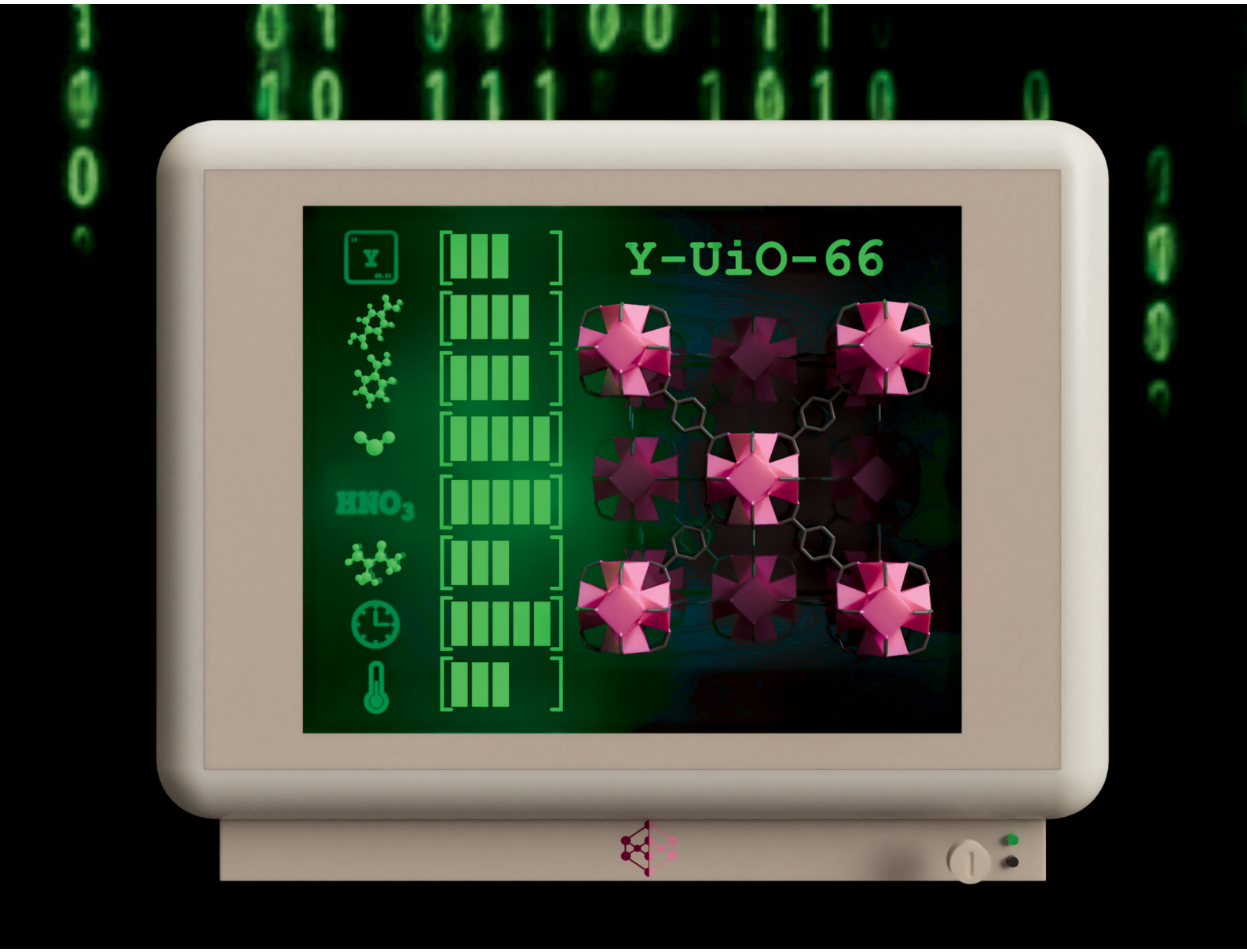

ISSN 2633-5409

ROYAL SOCIETY OF CHEMISTRY

PAPER
Ashlee J. Howarth *et al.*
Studying the significance of the parameters involved in the synthesis of Y-UiO-66 to improve product yield

Materials Advances

ROYAL SOCIETY OF CHEMISTRY

PAPER

View Article Online
View Journal | View Issue

Cite this: *Mater. Adv.*, 2026, 7, 2621

Studying the significance of the parameters involved in the synthesis of Y-UiO-66 to improve product yield

Micaela Richezzi, [a] P. Rafael Donnarumma[b] and Ashlee J. Howarth *[a]

The significance of the parameters involved in the synthesis of rare-earth metal–organic frameworks (RE-MOFs) has not been studied in depth. Design of experiments (DoE) is used herein to determine the impact of seven synthetic parameters on the yield and surface area of Y-UiO-66 (UiO = University of Oslo). The seven synthetic parameters are evaluated through 16 experiments, leading to a new synthetic procedure for Y-UiO-66 that increases the yield from 33% to 84% while maintaining high crystallinity and surface area. These results show that a simple screening design, using DoE, is useful for the improvement of MOF synthesis. The new procedure is successfully adapted to scale-up the reaction twenty times, as well as to improve the yield of Ho- and Yb-UiO-66, demonstrating that it can be extended to lanthanoid analogues of UiO-66. The results obtained from the design were used to improve the yield of another RE cluster-based MOF, Tb-CU-27 (CU = Concordia University) with only one experiment, suggesting that the synthetic parameters identified as being significant for Y-UiO-66 have a similar effect on other RE cluster-based MOFs.

Received 16th October 2025,
Accepted 4th February 2026

DOI: 10.1039/d5ma01198a

rsc.li/materials-advances

Introduction

Metal–organic frameworks (MOFs) are porous materials produced by the bridging of inorganic building units with multitopic organic ligands, or linkers, which act as organic building units.[1–6] The inorganic and organic components come together to form building blocks commonly termed secondary building units (SBUs).[7] The vast number of options for inorganic structures, organic linkers, and in turn, SBUs, constructs a virtually infinite MOF material space. It is due to their structural characteristics, such as permanent porosity and immense free volume with values up to 90%,[8] that several potential applications of MOFs have been explored. The potential applications include gas adsorption,[9–11] catalysis,[12–14] chemical sensing,[15–17] and water treatment,[18] among many others. A subset of MOFs are those containing rare-earth (RE) elements, meaning yttrium, scandium, and the *f*-block metals ranging from lanthanum to lutetium. There has been significant attention focused on the synthesis of RE-MOFs due to their attractive coordination chemistry, particularly the diversity in their coordination numbers and geometries, which can lead to a large library of possible SBUs for MOFs.[19–24]

Within the subset of RE-MOFs, the materials can be further classified by the identity of their SBUs taking the form of metal ions, chains, or clusters.[19] Although several RE cluster-based MOFs have been reported in the literature,[19,22–28] the synthetic processes required to obtain these MOFs have not been studied in-depth, particularly compared to *d*-block metal MOF analogues.[29–34] For instance, the synthesis of Zr-UiO-66 has been studied extensively to control defects in the structure,[35–37] improve yield,[38] and eliminate the use of DMF.[39,40] Furthermore, RE cluster-based MOFs are often synthesized on a small scale (< 15 mg)[17,41,42] and/or with low percent yields ($< 40\%$).[43–45] While small scale syntheses and low yields are sufficient for most fundamental academic studies, and to demonstrate a proof-of-concept, larger scale syntheses and higher yields are required to move the materials towards application.[46,47] As such, understanding the synthetic parameters that are significant in influencing the yield of RE cluster-based MOFs is important for scaling up their synthesis. However, improving MOF yield should not come at the cost of sample quality. It is thus critical to ensure that the crystallinity as well as porosity of the resulting MOFs is in line with reported results, as permanent porosity and BET surface area are important indicators of the quality of a MOF sample. Usually, when working to optimize a MOF synthetic procedure for yield and quality, the synthetic parameters are varied one at a time, in a

[a] *Department of Chemistry and Biochemistry and Centre for NanoScience Research, Concordia University, 7141 Sherbrooke Street West, Montreal, Quebec, H4B 1R6, Canada. E-mail: ashlee.howarth@concordia.ca*
[b] *CIC biomaGUNE, Parque Científico y Tecnológico de Gipuzkoa, Paseo Miramón 194, 20014, Donostia/San Sebastián, Gipuzkoa, Spain*

systematic way, until the process is improved. The disadvantage of this method is that the information obtained for one parameter might not be true after other synthetic parameters are studied. For instance, if the reaction time is studied first, while keeping the other parameters constant, the best reaction time under these conditions might not necessarily be the best reaction time once the other synthetic parameters are varied. Design of experiments (DoE) is a statistical technique that allows for the study of the effect of numerous factors (*i.e.*, synthetic parameters) on a desired response, simultaneously.[48] In the MOF field, DoE has been used to study the effect of the synthesis conditions on the oxygen sensitivity of Zr-MOFs,[49] and the particle size of Fe-MIL-88A,[50] among others.[51–53] However, it has never been employed to understand the effect of the synthetic parameters involved in the synthesis of RE-MOFs.

In a typical DoE screening design, six simple steps must be followed:[54]

(1) Selecting response variables: these are the properties of the resulting material to be measured and optimized. One of the advantages of DoE is that the same set of experiments can be used to study multiple response variables. In this study, yield and surface area are chosen as the response variables to optimize.

(2) Selecting the factors and levels: the factors are the synthetic parameters under study, and they usually vary between two levels in a screening design. In this study, temperature, time, and equivalents of precursors, solvents, and modulators are chosen as the factors.

(3) Selecting the type of design: this will depend on the number of factors, the number of experiments to be run, and the desired resolution, which dictates how many factors and interactions can be analysed. In this study, a 2^{7-3} design was chosen to limit the number of experiments required while still gaining the necessary information (*vide infra*).

(4) Running the design: in this step, the statistical software will give a list of experiments to be performed.

(5) Performing the experiments and measuring the response: in this study, focusing on optimizing yield and surface area, while maintaining high crystallinity.

(6) Analysing the results: in this study to create an improved synthetic procedure that improves yield while still leading to high quality samples.

Herein, we report the use of DoE to study the significance of various synthetic parameters on Y-UiO-66 and their effect on the yield and surface area of the resulting MOF. The information obtained is used to scale-up the reaction twenty times, while maintaining a high quality MOF. Additionally, the results are used to easily improve the yield of other RE cluster-based MOFs.

Results and discussion

Original synthesis and selection of synthetic parameters

The reported yield for the synthesis of Y-UiO-66 when using yttrium nitrate as a precursor is 39%.[45] However, there is always variability in the yield of MOF reactions that can be attributed to using different bottles of reagents (*i.e.*, different batches from the same supplier, or different suppliers), slight weight differences caused by human error, or factors such as room temperature and humidity level varying from day-to-day or location-to-location. For this reason, before starting the DoE, Y-UiO-66 was synthesized with the same reagents that were used for the entire study, while also limiting the weighing variability to ± 0.2 mg. Weighing reagents directly into the reaction vial also contributes to having a more exact weight, which is important for DoE in order to control the conditions as rigorously as possible. Having all these precautions in place, Y-UiO-66 was synthesized using the reported procedure (Fig. 1) in duplicate with yields of 28 and 31% (14.1 and 15.5 mg, respectively). When considering using MOFs in practical applications, it is important that the synthesis can be scaled up. However, scaling-up a reaction with such low yields (~30%) would lead to a great waste of resources. Consequently, before attempting a scale-up, it is important to optimize the yield.

While varying each synthetic parameter one-by-one in a systematic way can lead to optimized reaction conditions and improved yields, DoE has the advantage of saving time and resources by providing valuable information about the effect of each synthetic parameter on the yield, even when multiple synthetic parameters are varied at the same time.[54] As such, far more information can be gained about a synthetic process with far fewer experiments. Additionally, since one set of

Fig. 1 Scheme of the reported procedure for the synthesis of Y-UiO-66, which is used herein as a starting point for the DoE. Reagents: $Y(NO_3)_3{\cdot}xH_2O$, terephthalic acid (BDC), 2,6-difluorobenzoic acid (2,6-dFBA), *N*,*N*-dimethylacetamide (DMAc), H_2O and HNO_3.

Table 1 Factors under study with their respective levels

Factor	Lower level (−1)	Higher level (+1)
Temperature (°C)	120	130
Time (h)	24	48
Modulator (equivalents)	16	20
Linker (equivalents)	1	1.4
Co-modulator (equivalents)	9	13.5
Water (mL)	0.1	0.2
Solvent (mL)	4	8

experiments can be used to study numerous responses at the same time, it is possible to evaluate how to increase product yield while maintaining the quality of the material, simultaneously. One measurable response to assess the quality of a porous material is the surface area. The reported surface area for Y-UiO-66 using our standard procedure is 1060 m^2/g,[45] although batch-to-batch variability of +/− 15% is common with MOFs. For instance, following the reported procedure, a surface area as low as 940 $m^2\ g^{-1}$ has been obtained (Fig. S1). With this in mind, a surface area above 900 $m^2\ g^{-1}$ would be considered acceptable for Y-UiO-66 and can be set as the lower bound for the DoE response.

All the synthetic parameters for Y-UiO-66 were selected as factors for the DoE, and, in all cases, one of the levels corresponds to our standard reported synthetic condition (Table 1). The other level was selected based on previous results we obtained when trying to synthesize Y-UiO-66 for the first time,[25] or when modifying the procedure to obtain single crystals[55] or to use a different metal precursor.[45] These previous studies combined allowed us to understand the upper and lower limits in synthetic parameter variation that can still give Y-UiO-66 as a phase pure product. Since it is important that Y-UiO-66 is the primary product under all the DoE conditions, very drastic changes were avoided. Temperature was increased from 120 to 130 °C and time from 24 h to 48 h. Yttrium nitrate was kept as the limiting reagent, while the ratios of the other reagents and solvents were varied. The volume of dimethylacetamide (DMAc) was decreased from 8 mL to 4 mL, considering that a lower volume could be beneficial for the scale-up.[56] The higher level set for the terephthalic acid (H_2BDC) linker, 1.4 equivalents, was chosen based on its solubility in 4 mL of DMAc. The equivalents of modulator were increased from 16 to 20, knowing that much lower or much higher amounts of 2,6-difluorobenzoic acid (2,6-dFBA) can impact the reproducibility of the reaction or result in other products. We have previously reported that the yield of these reactions is higher when using 0.1 mL of water (compared to no water).[45] To study the effect of increasing amounts of water, the selected higher level was set to 0.2 mL. Finally, the amount of co-modulator (nitric acid) was allowed to vary by up to 50%, with the higher level set to 13.5 equivalents (from 9 equivalents).

Design of experiments

In order to study the effect of the aforementioned factors on the yield and surface area of Y-UiO-66, an appropriate design was selected. A full factorial design consists of running all the possible combinations of factor levels, resulting in a total number of experiments given by 2^n, with n being the number of factors.[54] Additionally, replicates are necessary for this system, as both responses present a high variability even when using the same conditions. Consequently, a full factorial design with duplicates would require 256 experiments ($2^7 \times 2$ replicates).

This number of experiments is expensive, inconvenient, unnecessary, and would not be an improvement from the standard approach of varying one parameter at a time. For these reasons, when studying a large number of factors, fractional factorial designs are commonly used for the screening stage.[57] In these designs, only a fraction of the possible combinations is studied, and, although some information will be lost, as long as the design resolution allows for the estimation of main effects and relevant interactions, the significance of the factors can still be evaluated. The number of effects that can be estimated is related to the degrees of freedom, which are calculated as the total number of experiments minus 1. A 2^{7-3} design was chosen, resulting in a total of 16 experiments carried out by duplicate. Since this design has 15 degrees of freedom, 7 factors and 8 interactions can be analysed. The list of experiments generated using the FrF2 package in R along with the experimentally obtained surface areas and product yields are detailed in Table S1 and Fig. S2.

In addition to the surface area and yield, the materials obtained in the 16 reactions were also characterized by powder X-ray diffraction (PXRD) and scanning electron microscopy (SEM). The PXRD patterns confirm that Y-UiO-66 was the primary product of all the reactions (Fig. S3). However, in some cases, additional peaks were observed around 6 and 10°2θ. The samples that present these impurity peaks were also the ones that exhibited lower surface areas, indicating that the quality of the material is inferior (Fig. S3–S5). For example, these peaks are most prevalent for reaction number 4, which is the material with the lowest surface area (326 $m^2\ g^{-1}$). The expected octahedral crystallites are observed in all the SEM images (Fig. S6), although it is noteworthy that some conditions seem to favour the formation of truncated octahedrons. It can be observed that other characteristics seem to be dependent on the synthetic conditions, such as crystallite size and the tendency of the crystallites to agglomerate, however these responses are not the focus of this study.

Another important observation made through performing the 16 reactions suggested for the DoE, is that the colour of the resulting Y-UiO-66 samples was not consistent in all the reactions (Fig. S7). Products from reactions number 1 and 15 have an intense yellow colour, and they also happen to have rather low surface areas (675 and 668 $m^2\ g^{-1}$). While the samples with the highest surface areas are white in colour (reactions 13 (1033 $m^2\ g^{-1}$) and 14 (1033 $m^2\ g^{-1}$)), the rest have pale yellow tones and surface areas varying from 326 to 968 $m^2\ g^{-1}$. These results suggest that if the yellow colour is caused by an impurity, it does not have a direct relationship with the surface area unless it is present in high amounts. The yellow Y-UiO-66 sample obtained from experiment number 1 was characterized by ^1H NMR spectroscopy and two additional peaks at 2.9 and

2.3 ppm were observed (Fig. S8 and Table S2). These peaks do not correspond to the MOF, and the one at 2.3 ppm was also observed in some white samples (see scale-up) and can be removed by washing the sample with methanol. As such, we hypothesize that the peak at 2.9 ppm is the one responsible for the yellow colour observed in some samples, and that it may be related to nitrosamine impurities, which can form when using metal nitrate precursors in amide-containing solvents.[58]

Analysis and selection of improved synthetic conditions

In order to determine the main factors that have a significant effect on the yield and surface area of Y-UiO-66, an Analysis of Variance (ANOVA) test was carried out and the obtained p-values are summarised in Table S3. A main factor has a significant effect on a particular response when the mean response for each level of that factor are different enough, and p-values are used to determine if their difference is sufficiently large. Factors with a p-value lower than the selected significance level ($\alpha = 0.05$) are considered to have a significant effect on the studied response. For yield, these factors include temperature (p-value = 2.96×0^{-3}), time (p-value = 1.64×10^{-3}), equivalents of linker (p-value = 0.0261), and volume of solvent (p-value = 0.0260). For surface area, the significant factors include temperature (p-value = 1.95×0^{-10}), time (p-value = 3.15×10^{-7}), equivalents of co-modulator (p-value = 0.0471), and volume of solvent (p-value = 0.0382). To select conditions for the ideal procedure where both yield and surface area are maximized, some of the interactions between factors need to be considered. Due to the alias structure of this fractional factorial design (given by the resolution), only eight interactions between factors can be analysed and three were determined to be significant for both responses (Table S4): the interaction between temperature and equivalents of modulator, the interaction between equivalents of modulator and equivalents of linker and the interaction between temperature and time. Taking all this information into account as well as the main effects and interactions plots (Fig. S9–S13), the final conditions were selected as follows:

(1) The equivalents of linker are only significant for yield, leading to an increase in the yield at the higher level. Since the surface area remains unchanged at both levels, the higher level (1.4 equivalents) was selected.

(2) While the equivalents of co-modulator are only significant for surface area, the higher level increases both responses and was selected for the final conditions (13.5 equivalents).

(3) Volume of water at the levels tested is not significant, and the level that increases the yield was selected (0.2 mL).

(4) Temperature is significant for both responses, but the effect is the opposite: while the higher temperature increases the yield, it leads to a large decrease in surface area. Consequently, this parameter was kept at 120 °C to maintain the quality of the material as high as possible.

(5) Time has a similar effect to temperature. However, it is important to consider the interaction between these two factors. At the selected temperature, going from 24 to 48 h produces a large increase in the yield, while it does not seem to affect the surface area as much. For this reason, 48 h was selected.

(6) Equivalents of modulator is not significant itself, but two interactions involving this factor are. Analysing the interactions plots, it can be observed that at the selected levels for equivalents of linker and temperature, the higher level of equivalents of modulator (20 equivalents) leads to both a higher yield and a higher surface area.

(7) Finally, the volume of solvent has opposite effects. While the higher level (8 mL) increases the yield, the lower (4 mL) increases the surface area. However, there is no information available about the significance of the interactions to assist this decision. To select this level, two experiments were performed where the other six factors were kept at the chosen levels (1–6 above) and the equivalents of solvent were varied. The results indicate that the higher level of solvent leads to slightly higher yields (average of 84% vs 78%) and surface areas (average of 1050 $m^2\ g^{-1}$ *vs.* 1035 $m^2\ g^{-1}$), as well as a whiter material (Fig. 2 and Fig. S14 and Table S5). As mentioned before, the yellow colour is attributed to an impurity that is also observed in the ^{1}H NMR spectrum of the sample using 4 mL of solvent (Fig. S15). For this reason, the conditions leading to a white pure sample were selected.

Y-UiO-66 synthesized using the DoE optimized procedure was further characterised by PXRD, SEM, ^{1}H NMR spectroscopy, and thermogravimetric analysis (TGA). The PXRD pattern corresponds to a crystalline material that is isostructural to Zr-UiO-66 with **fcu** topology, as expected, and all the peaks observed correspond to allowed reflections (Fig. 2, blue trace). The SEM images show truncated octahedrons with sizes between 1 and 20 μm (Fig. S16). The ^{1}H NMR spectrum of the digested sample exhibits the peak corresponding to the linker at 7.8 ppm (Fig. S17 and Table S6). The peaks at 3.5, 2.8 and 1.9 correspond to water, dimethylammonium, and acetate, as previously reported.[45] Moreover, the integrations of this sample (Table S6) and the reported one are the same, leading to a calculated formula containing five BDC linkers, $[(CH_3)_2NH_2]_{1.5}$-$[RE_6(\mu_3\text{-}X)_8(BDC)_5(C_2H_3O_2)_{1.5}]$, and a theoretical yttrium content of 32.9%. The experimental percentage of yttrium (36.3%) calculated from the residue of the TGA is in agreement with the theoretical value (Fig. S18).

Scale-up

An interesting and unexpected advantage of the DoE optimized procedure that is better for scale-up is that the MOF particles no longer stick to the glass reaction vessel, making them easier to retrieve and leading to a lower mass loss during the work-up. The 10× and 20× scale-up were attempted by using the conditions obtained with the design of experiments, with the masses and volumes multiplied by ten or twenty. The resulting MOF product was easy to retrieve as it was mostly suspended in the solution. 10 seconds of sonication were enough to ensure that no solid was adhered to the walls. The yield obtained was 82% (410 mg) and 84% (840 mg) for 10 and 20 times, respectively. The structure of the MOFs was confirmed by PXRD (Fig. S19), and the surface areas of 960 (10×) and 990 (20×) $m^2\ g^{-1}$ are in

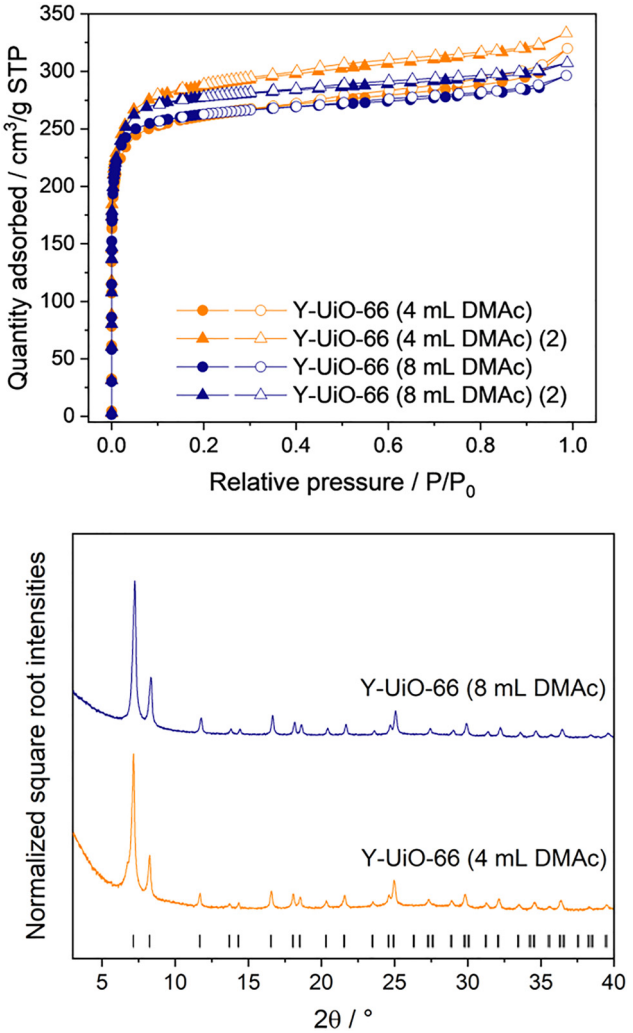

Fig. 2 N_2 adsorption–desorption isotherms (top) and PXRD patterns (bottom) of Y-UiO-66 obtained with six optimized parameters, but varying the volume of solvent. Closed circles and triangles correspond to adsorption and open correspond to desorption.

the expected range for Y-UiO-66 (Fig. S20). SEM images confirm the octahedral and truncated octahedral morphology with crystallite sizes between 1–20 μm (Fig. S21). It is noteworthy that, at first, surface areas of 870 and 880 $m^2\ g^{-1}$ were obtained, and a peak at 2.3 ppm was observed in the ^{1}H NMR spectra for the 10× and 20× scale Y-UiO-66 samples (Fig. S22 and Table S7). This impurity was most likely trapped in the pores and was removed by three additional washes with methanol. Considering the larger amount of Y-UiO-66 product obtained, it is possible that the products from the scaled-up procedure require more washing to remove all the impurities from the pores. The ^{1}H NMR spectra after washing the samples with methanol exhibit the expected peaks, with the same integrations as determined from the smaller batch synthesis, suggesting a comparable material was obtained (Fig. S23 and Table S7). TGA traces for the scaled-up Y-UiO-66 samples are similar to those obtained for samples from smaller batches (Fig. S24).

Application to other systems

The newly optimized procedure was used to synthesize Ho- and Yb-UiO-66 to determine if the same synthetic parameters are significant for yield and surface area in other RE-UiO-66 analogues. The yields for these MOFs were reported to be 31 and 23%, for Ho and Yb, respectively.[45] Following the new procedure, these yields increased to 88 and 82%, demonstrating that the results obtained for Y-UiO-66 using DoE can be applied to other RE-UiO-66 analogues containing lanthanoid ions. The PXRD patterns confirm the structure of the MOF (Fig. S25) and the obtained surface areas (890 $m^2\ g^{-1}$ for Ho-UiO-66 and 700 $m^2\ g^{-1}$ for Yb-UiO-66) are comparable to the ones reported (820 $m^2\ g^{-1}$ for Ho-UiO-66 and 650 $m^2\ g^{-1}$ for Yb-UiO-66),[45] confirming the high quality of the obtained materials (Fig. S26). The yields and BET surface areas of Y-UiO-66, Ho-UiO-66, and Yb-UiO-66 reported herein compared to our previous works[25,45,55] are summarized in Table S8.

This work succeeded in optimising the synthetic conditions used to obtain RE-UiO-66 and in showing how DoE can be used to improve MOF yield, while maintaining quality, by performing only a few experiments. It is of interest to determine whether the information obtained about this particular system (*i.e.*, RE-UiO-66) can be applied to other RE cluster-based MOFs. In other words, whether the factors (*i.e.*, synthetic parameters) that lead to an increase in yield for RE-UiO-66 can be directly used to improve the yield of another RE cluster-based MOF. To study this, we selected a Tb-MOF with **shp** topology (Tb-CU-27), comprised of nonanuclear cluster nodes and the 1,2,4,5-tetrakis(4-carboxyphenyl)benzene linker. Since the procedure reported in 2022 was performed on a very small scale,[26] we scaled it up two times. The yield obtained from the 2× scale of Tb-CU-27 was 4.2 mg (10%), which was too low to perform N_2 adsorption–desorption measurements.

Considering that the reported synthesis consists of leaving the reaction for 72 h at 120 °C, these factors were not modified to avoid a negative impact on the surface area and yield. Three synthetic parameters were increased based on previous DoE results for Y-UiO-66: the equivalents of linker (50%), the equivalents of modulator (10%) and the volume of solvent (52%). It is noteworthy that all these reagents are different from the ones used for the synthesis of RE-UiO-66 but should serve a similar purpose in the reaction. Using this newly optimized procedure, Tb-CU-27 was obtained with a yield of 18.3 mg (30%), more than 4× the mass obtained using the reported procedure.[26] The material was characterized by PXRD, confirming the structure of the MOF (Fig. S27). The BET surface area was 1310 $m^2\ g^{-1}$ (Fig. 3), which is comparable to the reported one (1365 $m^2\ g^{-1}$),[26] indicating that the new synthesis leads to a high-quality material while increasing the yield more than 4 times.

These results show that, although a DoE would give more precise and tailored conditions for each system, the information obtained for Y-UiO-66 can be used to improve the product yield of other RE cluster-based MOFs, while maintaining quality. By modifying some of the parameters that were found to be significant for Y-UiO-66, the yield of other RE cluster-based

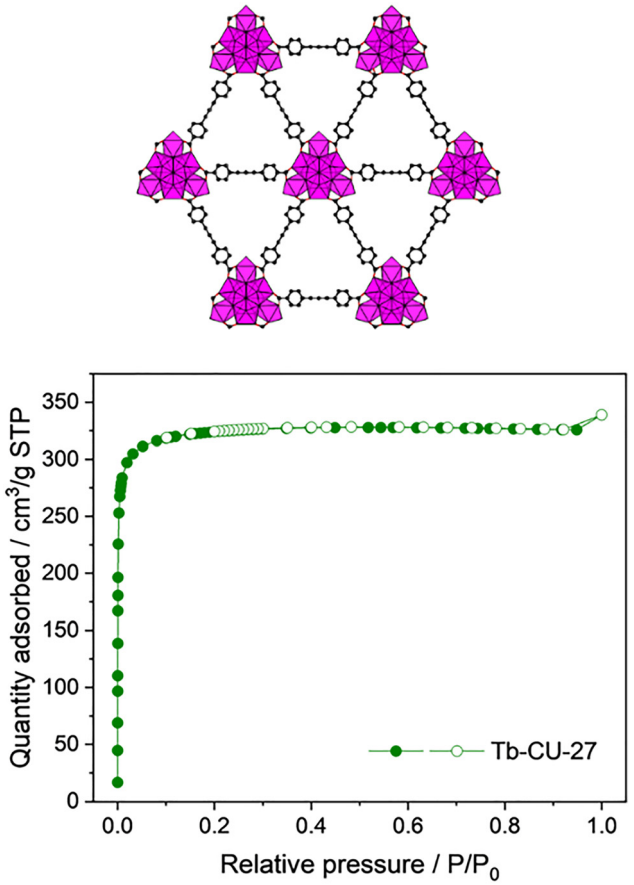

Fig. 3 Structure (top) and N_2 adsorption–desorption isotherm (bottom) of Tb-CU-27 synthesised using the newly optimized procedure adapted from the results obtained from the DoE for Y-UiO-66. Closed circles correspond to adsorption and open correspond to desorption.

MOFs can be increased quickly without performing more than a few experiments.

Conclusions

In summary, we have demonstrated that factorial designs can be used in a simple, fast, and economic way to obtain information about the most significant parameters involved in the synthesis of RE cluster-based MOFs. Furthermore, that information can be used to improve the MOF yield while maintaining high quality. The new synthesis of Y-UiO-66 increased the yield from 33% to 84% and allowed for an efficient 20× scale up, giving rise to 840 mg of MOF – the largest scale reported for a RE cluster-based MOF. This same procedure was successfully used to make Ho- and Yb-UiO-66, obtaining yields of 88 and 82%, compared to 31% and 23% for the previously reported syntheses. All the materials exhibited surface areas in the expected range, and were confirmed to be of high quality. Lastly, the information about the effect of the synthetic parameters on the yield of Y-UiO-66 was used to improve the yield of Tb-CU-27, another RE cluster-based MOF. In only one attempt, the yield was improved by more than 4×, suggesting that similar variations in synthetic parameters to those used for Y-UiO-66 can positively affect the yield of other RE cluster-based MOFs.

Experimental section

Synthesis of Y-UiO-66

The starting conditions used to synthesize Y-UiO-66 correspond to our reported procedure.[45] In a 6-dram vial, $Y(NO_3)_3{\cdot}xH_2O$ (65.0 mg, 0.170 mmol assuming hexahydrate), terephthalic acid (H_2BDC, 28.5 mg, 0.172 mmol), and 2,6-difluorobenzoic acid (2,6-dFBA, 440.0 mg, 2.78 mmol) were suspended in 8 mL of dimethylacetamide (DMAc). 0.1 mL of water and 0.1 mL of HNO_3 were added afterwards, and the mixture was sonicated until dissolution. The sealed vial was placed in a preheated oven at 120 °C for 24 hours. The white solid was then separated by centrifugation and washed 5 times with 8 mL of DMF over 48 hours and 4 times with 8 mL of acetone over 72 hours. The material was air dried, followed by activation at 80 °C under vacuum for 20 hours. Note: under these conditions, Y-UiO-66 forms on the walls of the 6-dram vial and needs to be suspended before washing with DMF and acetone. The MOF can be suspended (or removed from the vial walls) by sonication in the reaction medium or by gently scraping the vial walls with a stir rod.

Synthesis of Y-UiO-66 for DoE

The 16 reactions were performed by following the conditions given by the DoE software but keeping the work-up and activation from the original procedure. See Table 1 and S1 for details.

Improved synthesis of Y-UiO-66. In a 6-dram vial, $Y(NO_3)_3{\cdot}xH_2O$ (65.0 mg, 0.170 mmol assuming hexahydrate), terephthalic acid (40.0 mg, 0.241 mmol), and 2,6-difluorobenzoic acid (550.0 mg, 3.48 mmol) were suspended in 8 mL of dimethylacetamide. 0.2 mL of water and 0.15 mL of HNO_3 were added afterwards, and the mixture was sonicated until dissolution. The sealed vial was placed in a preheated oven at 120 °C for 48 hours. The white solid was separated by centrifugation and washed 4 times with 8 mL of DMF over 48 hours, 3 times with 8 mL of methanol over 24 hours and 2 times with 8 mL of acetone over 48 hours. The material was air dried, followed by activation at 80 °C under vacuum for 20 hours. Note: under these conditions, Y-UiO-66 does not form on the walls of the vial. This same procedure was used for the synthesis of Ho- and Yb-UiO-66.

Scale-up of Y-UiO-66. In a 250 mL reaction jar, $Y(NO_3)_3{\cdot}xH_2O$ (650 mg, 1.70 mmol assuming hexahydrate), terephthalic acid (400.0 mg, 2.41 mmol), and 2,6-difluorobenzoic acid (5.50 g, 34.8 mmol) were suspended in 80 mL of dimethylacetamide. 2.0 mL of water and 1.5 mL of HNO_3 were added afterwards, and the mixture was sonicated until dissolution. The sealed jar was placed in a preheated oven at 120 °C for 48 hours. The white solid was separated by centrifugation and washed 4 times with 25 mL of DMF over 48 hours, 3 times with 25 mL of methanol over 24 hours and 2 times with 25 mL of acetone over 72 hours. The material was air dried, followed by activation at

80 °C under vacuum for 20 hours. The 20× scale up was performed following the same procedure, doubling the quantities.

Synthesis of Tb-CU-27. The reported synthesis was scaled-up 2× as a control.[26] In the new synthesis, $Tb(NO_3)_3{\cdot}xH_2O$ (0.1474 mmol, 64.0 mg), 1,2,4,5-tetrakis(4-carboxylphenyl)benzene (H_4TCPB, 0.0358 mmol, 20.0 mg) and 2-fluorobenzoic acid (2-FBA, 15.7 mmol, 2200 mg) were weighed in an 8-dram vial. The solids were suspended in 20.0 mL of DMF, and 3.0 mL of acetic acid were added. The mixture was sonicated until dissolution and placed in a preheated oven at 120 °C for 72 hours. The crystals were separated by centrifugation and washed 3 times with DMF over 48 hours and 3 times with methanol over 48 hours. The material was air dried, followed by activation at 120 °C under vacuum for 24 hours.

Design of experiments. The fractional factorial design (2^{7-3}, resolution IV) was generated using the FrF2 R package on RStudio (v4.3.1; R Core Team 2023).[59,60] The results were analyzed using the Analysis of Variance (ANOVA) test as well as main effects and interaction plots, also using RStudio.

Author contributions

Micaela Richezzi: conceptualization, formal analysis, investigation, validation, methodology, visualization, writing – original draft, writing – review & editing. P. Rafael Donnarumma: conceptualization, visualization. Ashlee J. Howarth: conceptualization, methodology, funding acquisition, resources, supervision, writing – review & editing.

Conflicts of interest

There are no conflicts to declare.

Data availability

Data for this article, including raw files for PXRD, N_2 gas sorption, and TGA, are available at borealis: The Canadian Dataverse Repository at https://doi.org/10.5683/SP3/POD6IH.

Supplementary information (SI): nitrogen adsorption–desorption isotherms, PXRD, NMR spectra, SEM images, and details on the design of experiments. See DOI: https://doi.org/10.1039/d5ma01198a.

Acknowledgements

MR thanks Concordia University for a Graduate Doctoral Fellowship. We acknowledge the support of the Natural Sciences and Engineering Research Council of Canada (NSERC), [funding reference number: RGPIN-2024-04293]. Cette recherche a été financée parle Conseil de recherches en sciences naturelles et en génie du Canada (CRSNG), [numéro de reference: RGPIN-2024-04293]. We acknowledge the support of the Canada Foundation for Innovation (CFI) and the Ministère de l'Enseignement supérieur (MES) [application number: 43646]. All MOF figures were made using VESTA 3.

Notes and references

1 A. J. Howarth, A. W. Peters, N. A. Vermeulen, T. C. Wang, J. T. Hupp and O. K. Farha, *Chem. Mater.*, 2016, **29**, 26–39.
2 B. F. Hoskins and R. Robson, *J. Am. Chem. Soc.*, 1989, **111**, 5962–5964.
3 O. M. Yaghi, G. Li and H. Li, *Nature*, 1995, **378**, 703–706.
4 O. M. Yaghi and H. Li, *J. Am. Chem. Soc.*, 1995, **117**, 10401–10402.
5 A. K. Cheetham, G. Férey and T. Loiseau, *Angew. Chem., Int. Ed.*, 1999, **38**, 3268–3292.
6 M. Kondo, T. Yoshitomi, H. Matsuzaka, S. Kitagawa and K. Seki, *Angew. Chem.*, 1997, **36**, 1725–1727.
7 O. M. Yaghi, M. O'Keeffe, N. W. Ockwig, H. K. Chae, M. Eddaoudi and J. Kim, *Nature*, 2003, **423**, 705–714.
8 H. Furukawa, N. Ko, Y. B. Go, N. Aratani, S. B. Choi, E. Choi, A. Ö. Yazaydin, R. Q. Snurr, M. O'Keeffe and J. Kim, *Science*, 2010, **329**, 424–428.
9 S. Ma and H.-C. Zhou, *J. Am. Chem. Soc.*, 2006, **128**, 11734–11735.
10 J. A. Mason, M. Veenstra and J. R. Long, *Chem. Sci.*, 2014, **5**, 32–51.
11 B. Zheng, J. Bai, J. Duan, L. Wojtas and M. J. Zaworotko, *J. Am. Chem. Soc.*, 2011, **133**, 748–751.
12 C. Wang, B. An and W. Lin, *ACS Catal.*, 2018, **9**, 130–146.
13 K.-I. Otake, Y. Cui, C. T. Buru, Z. Li, J. T. Hupp and O. K. Farha, *J. Am. Chem. Soc.*, 2018, **140**, 8652–8656.
14 D. Yang and B. C. Gates, *ACS Catal.*, 2019, **9**, 1779–1798.
15 T. Feng, Y. Ye, X. Liu, H. Cui, Z. Li, Y. Zhang, B. Liang, H. Li and B. Chen, *Angew. Chem.*, 2020, **132**, 21936–21941.
16 J. Ren, Z. Niu, Y. Ye, C. Y. Tsai, S. Liu, Q. Liu, X. Huang, A. Nafady and S. Ma, *Angew. Chem., Int. Ed.*, 2021, **60**, 23705–23712.
17 T.-Y. Luo, P. Das, D. L. White, C. Liu, A. Star and N. L. Rosi, *J. Am. Chem. Soc.*, 2020, **142**, 2897–2904.
18 A. J. Howarth, Y. Liu, J. T. Hupp and O. K. Farha, *CrystEngComm*, 2015, **17**, 7245–7253.
19 F. Saraci, V. Quezada-Novoa, P. R. Donnarumma and A. J. Howarth, *Chem. Soc. Rev.*, 2020, **49**, 7949–7977.
20 C. Daiguebonne, N. Kerbellec, O. Guillou, J.-C. Bünzli, F. Gumy, L. Catala, T. Mallah, N. Audebrand, Y. Gérault and K. Bernot, *Inorg. Chem.*, 2008, **47**, 3700–3708.
21 D.-X. Xue, A. J. Cairns, Y. Belmabkhout, L. Wojtas, Y. Liu, M. H. Alkordi and M. Eddaoudi, *J. Am. Chem. Soc.*, 2013, **135**, 7660–7667.
22 D. Alezi, A. M. P. Peedikakkal, Ł. J. Weseliński, V. Guillerm, Y. Belmabkhout, A. J. Cairns, Z. Chen, Ł. Wojtas and M. Eddaoudi, *J. Am. Chem. Soc.*, 2015, **137**, 5421–5430.
23 B. Al-Mohammadi, J.-X. Wang, H. Jiang, P. Parvatkar, A. Shkurenko, P. M. Bhatt, N. Y. Tashkandi, O. Shekhah, O. F. Mohammed and M. Eddaoudi, *ACS Appl. Mater. Interfaces*, 2024, **17**, 17751–17756.
24 E. Loukopoulos, G. K. Angeli, C. Tsangarakis, E. Traka, K. G. Froudas and P. N. Trikalitis, *Chem. – Eur. J.*, 2024, **30**, e202302709.
25 P. R. Donnarumma, S. Frojmovic, P. Marino, H. A. Bicalho, H. M. Titi and A. J. Howarth, *Chem. Commun.*, 2021, **57**, 6121–6124.

26 Z. Ajoyan, G. A. Mandl, P. R. Donnarumma, V. Quezada-Novoa, H. A. Bicalho, H. M. Titi, J. A. Capobianco and A. J. Howarth, *ACS Mater. Lett.*, 2022, **4**, 1025–1031.
27 V. Quezada-Novoa, H. M. Titi, A. A. Sarjeant and A. J. Howarth, *Chem. Mater.*, 2021, **33**, 4163–4169.
28 X.-L. Lv, L. Feng, L.-H. Xie, T. He, W. Wu, K.-Y. Wang, G. Si, B. Wang, J.-R. Li and H.-C. Zhou, *J. Am. Chem. Soc.*, 2021, **143**, 2784–2791.
29 C. Zheng, H. F. Greer, C.-Y. Chiang and W. Zhou, *CrystEngComm*, 2014, **16**, 1064–1070.
30 G.-T. Vuong, M.-H. Pham and T.-O. Do, *CrystEngComm*, 2013, **15**, 9694–9703.
31 O. O. Semivrazhskaya, D. Salionov, A. H. Clark, N. P. Casati, M. Nachtegaal, M. Ranocchiari, S. Bjelić, R. Verel, J. A. van Bokhoven and V. L. Sushkevich, *Small*, 2023, **19**, 2305771.
32 M. R. DeStefano, T. Islamoglu, S. J. Garibay, J. T. Hupp and O. K. Farha, *Chem. Mater.*, 2017, **29**, 1357–1361.
33 Z. Chen, L. Feng, L. Liu, P. M. Bhatt, K. Adil, A. H. Emwas, A. H. Assen, Y. Belmabkhout, Y. Han and M. Eddaoudi, *Langmuir*, 2018, **34**, 14546–14551.
34 S. Bauer, C. Serre, T. Devic, P. Horcajada, J. Marrot, G. Férey and N. Stock, *Inorg. Chem.*, 2008, **47**, 7568–7576.
35 Y. Feng, Q. Chen, M. Jiang and J. Yao, *Ind. Eng. Chem. Res.*, 2019, **58**, 17646–17659.
36 G. C. Shearer, S. Chavan, J. Ethiraj, J. G. Vitillo, S. Svelle, U. Olsbye, C. Lamberti, S. Bordiga and K. P. Lillerud, *Chem. Mater.*, 2014, **26**, 4068–4071.
37 M. A. Artsiusheuski, N. P. Casati, A. H. Clark, M. Nachtegaal, R. Verel, J. A. van Bokhoven and V. L. Sushkevich, *Angew. Chem., Int. Ed.*, 2025, **64**, e202415919.
38 F. Ragon, P. Horcajada, H. Chevreau, Y. K. Hwang, U.-H. Lee, S. R. Miller, T. Devic, J.-S. Chang and C. Serre, *Inorg. Chem.*, 2014, **53**, 2491–2500.
39 H.-Y. Chi, S. Song, K. Zhao, K.-J. Hsu, Q. Liu, Y. Shen, A. F. Sido Belin, A. Allaire, R. Goswami and W. L. Queen, *J. Am. Chem. Soc.*, 2025, **147**, 7255–7263.
40 N. Hosadoddi Srikantamurthy, J. F. Olorunyomi, C. M. Doherty, P. C. Sherrell and X. Mulet, *Adv. Sustainable Syst.*, 2025, **9**, e00854.
41 X. L. Lv, L. Feng, K. Y. Wang, L. H. Xie, T. He, W. Wu, J. R. Li and H. C. Zhou, *Angew. Chem., Int. Ed.*, 2021, **60**, 2053–2057.
42 T. Xia, Y. Wan, Y. Li and J. Zhang, *Inorg. Chem.*, 2020, **59**, 8809–8817.
43 E. Loukopoulos, G. K. Angeli, K. Kouvidis, C. Tsangarakis and P. N. Trikalitis, *ACS Appl. Mater. Interfaces*, 2022, **14**, 22242–22251.
44 G. K. Angeli, E. Loukopoulos, K. Kouvidis, A. Bosveli, C. Tsangarakis, E. Tylianakis, G. Froudakis and P. N. Trikalitis, *J. Am. Chem. Soc.*, 2021, **143**, 10250–10260.
45 M. Richezzi, P. R. Donnarumma, C. Copeman and A. J. Howarth, *Chem. Commun.*, 2024, **60**, 5173–5176.
46 M. Nazari, F. Zadehahmadi, M. M. Sadiq, A. L. Sutton, H. Mahdavi and M. R. Hill, *Commun. Mater.*, 2024, **5**, 170.
47 A. M. Wright, M. T. Kapelewski, S. Marx, O. K. Farha and W. Morris, *Nat. Mater.*, 2025, **24**, 178–187.
48 E. M. Williamson, Z. Sun, L. Mora-Tamez and R. L. Brutchey, *Chem. Mater.*, 2022, **34**, 9823–9835.
49 T. Burger, M. V. Hernandez, C. Carbonell, J. Rattenberger, H. Wiltsche, P. Falcaro, C. Slugovc and S. M. Borisov, *ACS Appl. Nano Mater.*, 2022, **6**, 248–260.
50 E. Bagherzadeh, S. M. Zebarjad, H. R. M. Hosseini and P. Chagnon, *CrystEngComm*, 2019, **21**, 544–553.
51 Q. Yu, H. V. Doan, Y. Xia, X. Hu, Y. Zhu, V. P. Ting, M. Taheri and M. Tian, *Int. J. Hydrogen Energy*, 2024, **81**, 371–381.
52 T. Zelenka, M. Balaz, M. Ferova, P. Diko, J. Bednarcik, A. Kiralyova, L. Zauska, R. Bures, P. Sharda, N. Kiraly, A. Badac, J. Vyhlidalova, M. Zelinska and M. Almasi, *Sci. Rep.*, 2024, **14**, 15386.
53 C. Sun, M. Barton, C. M. Pask, M. Edokali, L. Yang, A. J. Britton, S. Micklethwaite, F. Iacoviello, A. Hassanpour, M. Besenhard, R. Drummond-Brydson, K.-J. Wu and S. M. Collins, *Chem. Eng. J.*, 2023, **474**, 145892.
54 D. C. Montgomery, *Design and analysis of experiments*, John wiley & sons, 2017.
55 P. R. Donnarumma, C. Copeman, M. Richezzi, J. Sardilli, H. M. Titi and A. J. Howarth, *Cryst. Growth Des.*, 2024, **24**, 1619–1625.
56 R. T. Jerozal, T. A. Pitt, S. N. MacMillan and P. J. Milner, *J. Am. Chem. Soc.*, 2023, **145**, 13273–13283.
57 R. F. Gunst and R. L. Mason, *Wiley Interdiscip. Rev. Comput. Stat.*, 2009, **1**, 234–244.
58 J. C. Donovan, K. R. Wright and A. J. Matzger, *Angew. Chem.*, 2025, **137**, e202500531.
59 U. Grömping, *J. Stat. Softw.*, 2014, **56**, 1–56.
60 *RCoreTeam, R: A Language and Environment for Statistical Computing, V4.3.1*, R Foundation for Statistical Computing, Vienna, Austria, 2023, https://www.R-project.org/.